Microgravity Science and Technology (2022) 34: 42
https://doi.org/10.1007/s12217-022-09963-2

ORIGINAL ARTICLE

Experimental Study on Thermal Convection in Annular Pools Heated from Inner Cylinder

Qin Shu[1] · Dong-Ming Mo[2] · Li Zhang[3] · Jia-Jia Yu[1] · Chun-Mei Wu[1] · You-Rong Li[1]

Received: 5 December 2021 / Accepted: 19 May 2022 / Published online: 3 June 2022

Abstract

In order to understand the effect of the radius ratio on thermocapillary-buoyancy convection, a series of experimental observations on thermocapillary-buoyancy convection of 0.65cSt and 1cSt silicone oils have been conducted in annular pools with a smaller heating inner cylinder and the radius ratio of 0.25. The results show that the rotating petal-like structure or spoke pattern first appears on the free surface when thermocapillary-buoyancy convection destabilizes. As the Marangoni number increases, the spoke pattern becomes oscillating at the depth of 6–7 mm and the oscillating frequency is decreased compared with the results in the liquid pool with a radius ratio of 0.5. The wavenumber of the flow pattern decreases when the radius ratio decreases from 0.5 to 0.25. Especially at the liquid depth of 7–8 mm, a mode switching of the flow patterns has been observed and the flow pattern becomes more like cellular structures in cylindrical pools instead of the spoke pattern with the increasing Marangoni number. With the increase of the Prandtl number, this flow transition becomes difficult. Besides, the short spokes appear near the inner cylinder at a large Marangoni number and the deep fluid layer. Based on the experimental results, the general relationship of the threshold complex with the dynamic Bond number and the radius ratio is achieved.

Keywords Thermocapillary-buoyancy convection · Flow pattern · Radius ratio · Annular pool · Experiment

Nomenclature

Γ	Aspect ratio
d	Fluid layer depth, mm
m	Wavenumber
Ma	Marangoni number
Pr	Prandtl number
r	Radius, mm
g	Gravitational acceleration, m/s^2
T	Temperature, ℃

Greek symbols

α	Thermal diffusivity, m^2/s
γ_T	Temperature coefficient of surface tension, N/(m•K)
η	Radius ratio
μ	Dynamic viscosity of the fluid, kg/(m·s)
ν	Kinematic viscosity of the fluid, m^2/s
β	Thermal expansion coefficient, 1/K
ρ	Density, kg/m^3

Subscripts

cri	Critical
i	Inner
o	Outer

✉ You-Rong Li
liyourong@cqu.edu.cn

[1] Key Laboratory of Low-Grade Energy Utilization Technologies and Systems of Ministry of Education, College of Power Engineering, Chongqing University, Chongqing 400044, China

[2] Department of Mechanical Engineering, Chongqing Industry Polytechnic College, Chongqing 401120, China

[3] Chongqing City Management College, Chongqing 401331, China

Introduction

Under a normal gravity environment, even if a small tangential temperature gradient is applied in a liquid layer with a free surface, the coupling of surface-tension gradient and buoyancy can drive the fluid flow and form thermocapillary-buoyancy convection. When the thermocapillary-buoyancy convection destabilizes, several flow patterns can be observed, which has attracted the interest of many scientists from fundamental research (Qin et al. 2015) to industrial applications (Schwabe et al. 1978; Malyuk and Ivanova 2017; Savino et al. 2007). During the process of crystal growth, thermocapillary-buoyancy convection destabilization could make the properties of the crystal become uneven

and finally affect the crystal quality. Miller and Pernell (1982) performed an experiment to simulate the crystal growth process of gadolinium gallium garnet and observed the spoke pattern on the free surface. It was found that the wavenumber of the spoke pattern varies directly with the temperature difference. They speculated that the formation of spoke patterns could be attributed to the surface-tension gradient and buoyancy.

Recently, some researchers performed microgravity experiments to analyze the effect of buoyancy on flow patterns. Kamotani et al. (2000) conducted a series of experiments on thermocapillary convection of 2cSt silicone oil in annular containers onboard the USML-2 Spacelab. It was found that the two-lobed rotating or pulsating pattern appears on the free surface when the flow destabilizes. Schwabe et al. (2003) performed some experiments on thermocapillary convection of 0.65cSt silicone oil aboard the Russian satellite FOTON-12 and observed the oscillating multicellular flow and the traveling waves. Comparing the microgravity with terrestrial experimental results, Benz and Schwabe (2001) found that there is no proof to validate the existence of the spoke pattern in microgravity environment. They speculated that the formation of the spoke pattern is because the gravity suppresses the flow pattern transition to time-dependent mode. Shi et al. (2009) simulated thermocapillary convection of 0.65cSt silicone oil in annular pools under microgravity or normal gravity condition. It was found that thermocapillary-buoyancy convection destabilization could be suppressed by the buoyancy effect.

Considered the complex interaction between the thermocapillary stress and buoyancy, previous researchers defined a dynamic Bond number to describe their relationship. When the dynamic Bond number is less than 1, Garnier et al. (2006) reported that two kinds of hydrothermal waves appeared on the free surface of the annular pool. While the dynamic Bond number is more than 1, Favre et al. (1997) and Li et al. (2018) observed the petal-like structure and the spoke pattern in thermocapillary-buoyancy convection in Czochralski configuration. Shu et al. (2021) discussed the relationship between the petal-like structure and the spoke pattern, and found that the transition from the petal-like structure to the spoke pattern could be attributed to the Bénard-Marangoni instability. Jing et al. (2003) conducted a set of three-dimensional numerical simulations on the thermal convection of $LiNbO_3$ melt with a free surface in a cylindrical vessel and found that the Marangoni instability is the primary reason for generating the spoke pattern.

Nowadays, as a typical physical model similar to Czochralski crystal growth method, the annular pool has been widely used in experiments and numerical simulations to investigate thermocapillary-buoyancy convection. Previous works mainly focus on the effects of the aspect ratio (Liu et al. 2019a; Mo et al. 2021), Prandtl number (Liu et al. 2019b), the heating modes (Shu et al. 2021), the capillary ratio (Yu et al. 2016), the pool rotation (Shi et al. 2006) and the surface heat dissipation (Zhang et al. 2017) on the flow patterns in annular pools with the radius ratio of 0.5. A few works (Imaishi et al. 2020; López-Núñez et al. 2020) have investigated the flow patterns and their transition in annular pools with different radius ratios. As the radius ratio increases from 0.5 to 0.98039, Imaishi et al. (2020) found that the wavenumber of three-dimensional stable flow increases, and the wave shape becomes almost straight. When the radius ratio is less than 0.5, however, the variations of the thermocapillary-buoyancy convection with the radius ratio are yet unknown, which is important to understand the formation mechanism and evolution of flow patterns. This paper presented a series of experimental observations on the flow pattern of thermocapillary-buoyancy convection in annular pools when the radius ratio is decreased to 0.25. By comparing with the experimental results in annular pools with the radius ratio of 0.5 (Shu et al. 2021), the effects of radius ratio on the critical Marangoni number of the flow transitions and the flow pattern have been discussed.

Experimental Setup and Method

Experimental Setup

The annular pool is one of the typical experimental models to study thermocapillary-buoyancy convection under terrestrial conditions. As depicted in Fig. 1, the annular pool is

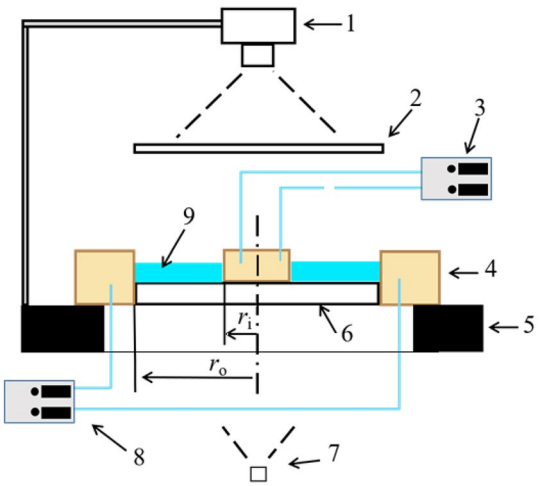

Fig. 1 The experimental setup. 1–Digital camera; 2–Screen; 3 – Thermostatic hot-water bath; 4 – Annular pool; 5–Vibration reduction platform; 6 – Plexiglass; 7–Point light source; 8–Cooling water bath; 9 – Silicone oil

composed of red copper, whose thermal conductive performance is pretty good. The annular pool has an inner radius of $r_i = 10 \pm 0.1$ mm and an outer radius of $r_o = 40 \pm 0.1$ mm. The depth of the liquid layer varies from $d = 4$ mm to $d = 8$ mm. To impose a radial temperature difference between the inner and outer cylinders, two thermostatic baths with the precision of $\pm$ 0.1 ℃ are used to maintain the inner and outer cylinders respectively at stationary temperatures T_i and T_o ($T_i > T_o$). Eight T-type thermocouples with the wire diameter of 127 μm are inserted through tiny holes into the inner and outer cylinders, respectively, to measure the cylinder temperatures, as shown in Fig. 2. The temperature fluctuation on the free surface is monitored using a T-type micro-thermocouple (OMEGA COCO-002) with the wire diameter of 50 μm positioned between these two cylinders. The sampling frequency is 5 Hz. Temperature data is processed by the data acquisition system (DAQ 34972A produced by Keysight Technologies) and recorded in the computer system. Considering the influence of environmental vibration on the flow pattern visualization experiment, the annular pool is placed on the vibration reduction platform. To facilitate the observation of the flow pattern, the transparent and adiabatic plexiglass with a thickness of 10 ± 0.1 mm is applied for the bottom of the annular pool. Transparent KF96 silicone oils of 0.65cSt and 1cSt are served as the working liquids. Their physical properties can be referred to in the previous work (Shu et al. 2021).

During the experimental processes, the laboratory room always maintains a dark and constant temperature of 25 ℃. The inner and outer cylinders of the annular pool are treated with 3 M EGC-1700 to avoid the influence of the meniscus on the flow patterns. Considering that the evaporation could change the fluid layer depth especially for 0.65cSt silicone oil, every experiment is completed within five minutes. In addition, another working liquid (1cSt silicone oil) which rarely evaporates in atmosphere condition is used to validate the influence of the fluid depth on the flow patterns. The fluid layer depth d ranges from 4 to 8 mm and the temperature difference between the inner and outer cylinders is controlled at no more than 50 ℃.

The radius ratio η, the Marangoni number Ma, the dynamic Bond number Bd, and the aspect ratio Γ, are respectively defined as

$$\eta = \frac{r_i}{r_o} \tag{1}$$

$$Ma = \frac{\gamma_T (T_i - T_o)(r_o - r_i)}{\mu\alpha}\Gamma^2 \tag{2}$$

$$Bd = \frac{\rho g \beta d^2}{\gamma_T} \tag{3}$$

$$\Gamma = \frac{d}{(r_o - r_i)} \tag{4}$$

Flow Pattern Visualization Method

The flow pattern visualization system consists of a point light source, transparent plexiglass, a screen, and a digital camera. The principle of the flow pattern visualization is that the refraction index of the working liquids varies with the temperature. When the basic flow transits to the three-dimensional stationary flow, the flow pattern can be observed on the screen if the light emitted from the point light source passes through the plexiglass and the working liquid. The light generated by a medical cold light source is directly transmitted through the optical cable and forms the point light source under the annular pool. The flow pattern can be recorded by the digital camera above the screen in real-time and saved on a computer. At a small temperature difference, thermocapillary-buoyancy convection is two-dimensional stable axisymmetric, and there is no flow pattern to be observed. Once the temperature difference (Marangoni number) is beyond a critical value, the basic flow transits to the three-dimensional stable or unstable flow, and the flow pattern appears as the petal-like structure and the spoke pattern.

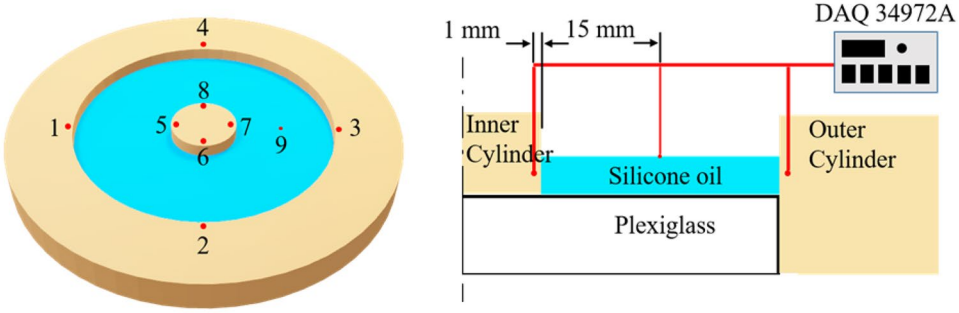

Fig. 2 The detailed temperature measuring system. 1,2,3,4,5,6,7, and 8–eight thermocouples with the wire diameter of 127 μm; 9–micro-thermocouple with the wire diameter of 50 μm

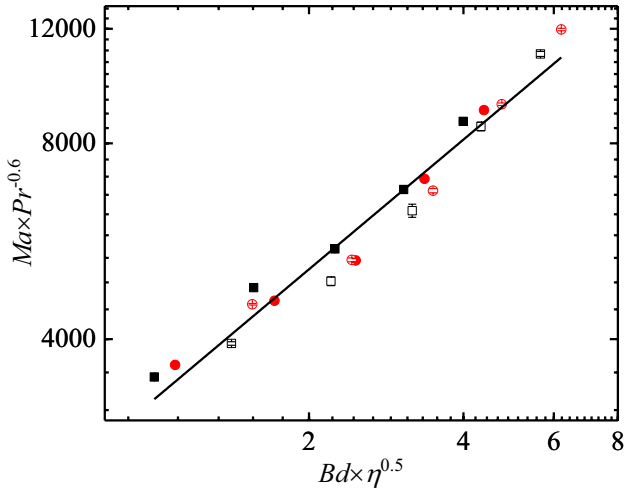

Fig. 3 Variations of the threshold complex $Ma \times Pr^{-0.6}$ with the dynamic Bond number and the radius ratio. Solid symbols: the present results; hollow symbols: values of Shu et al. (2021). Square: $Pr = 6.7$; circle: $Pr = 16.1$. The black solid line indicates the fitting line

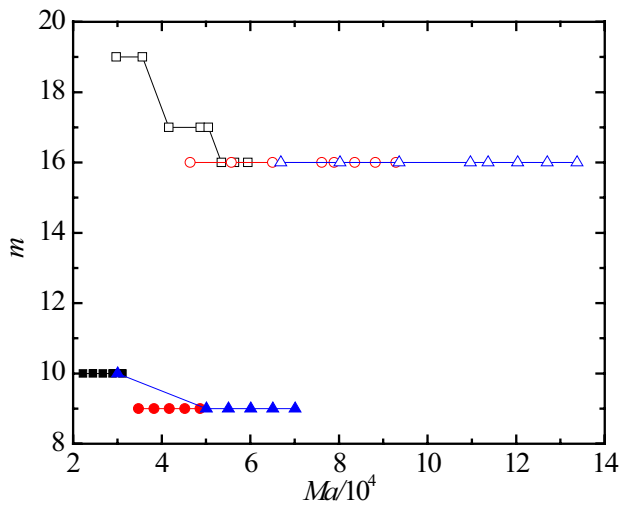

Fig. 5 Variation of the wavenumber with the Marangoni number for 0.65 cSt silicone oil. Solid symbols: the present results; hollow symbols: values of Shu et al. (2021). Square: $d = 4$ mm; circle: $d = 5$ mm; triangle: $d = 6$ mm

Results and Discussion

During the present and previous experiments (Shu et al. 2021), the fluids with the same Prandtl number are used to investigate the dependencies of the threshold Marangoni number on some control dimensionless parameters, such as the Prandtl number, the dynamic Bond number, and the radius ratio. It can be found that the threshold Marangoni number increases

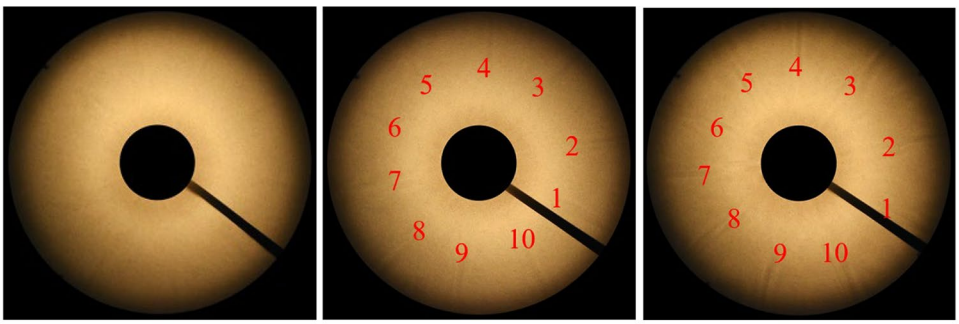

(i) ΔT=25℃ (Ma=2.2×10^4) (ii) ΔT=30℃ (Ma=2.7×10^4) (iii) ΔT=35 ℃ (Ma=3.1×10^4)

(a) d=4 mm (Bd=2.00)

(i) ΔT=25℃ (Ma=3.5×10^4) (ii) ΔT=30℃ (Ma=4.2×10^4) (iii) ΔT=35℃ (Ma=4.9×10^4)

(b) d=5 mm (Bd=3.12)

Fig. 4 The evolution of the surface temperature fields with the temperature difference (Marangoni number) at $Pr = 6.7$

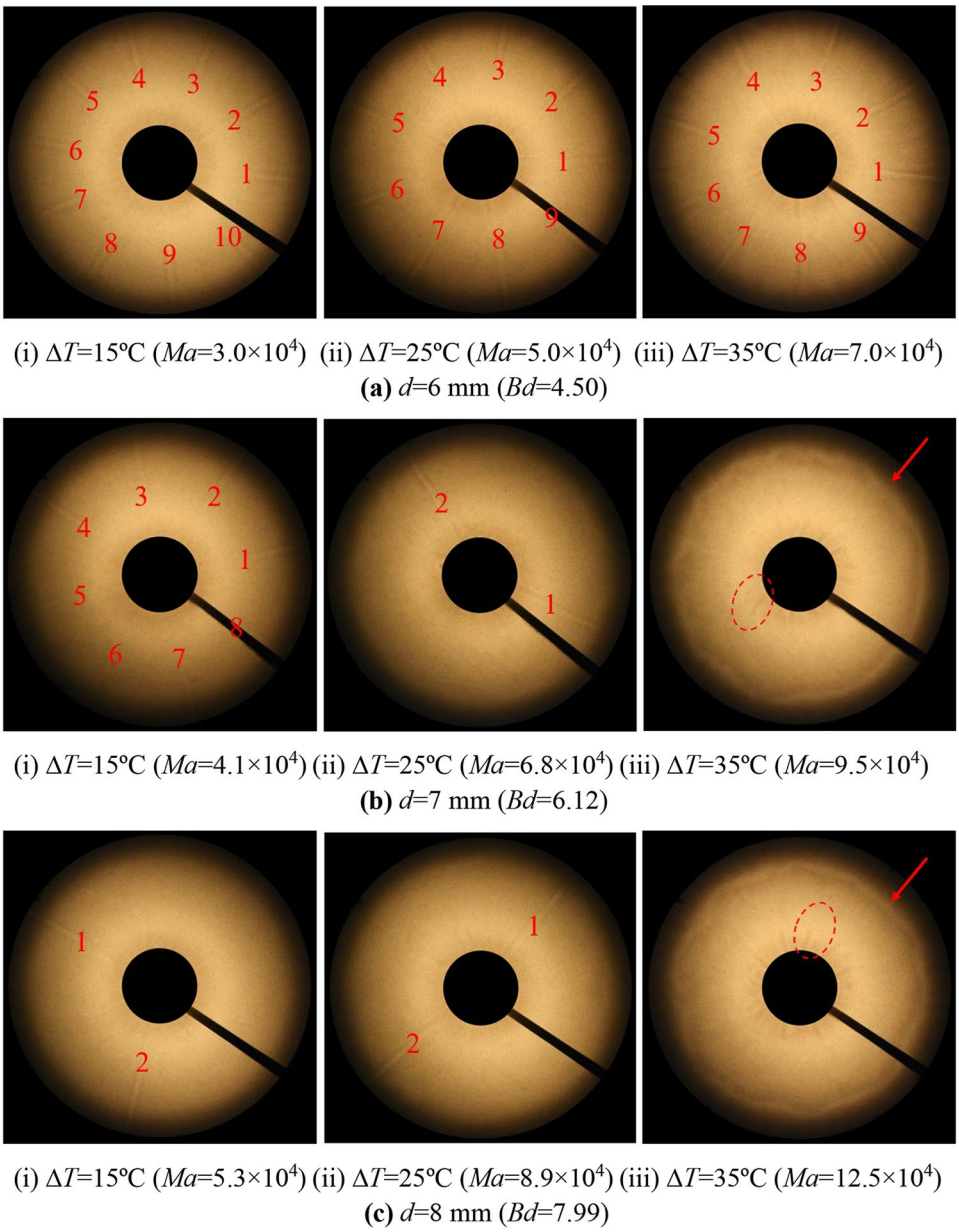

Fig. 6 Evolution of the surface temperature fields with the radial temperature difference (Marangoni number) at $Pr = 6.7$

with the increase of the aspect ratio and the Prandtl number, which agrees with the previous work with a large inner radius (Shu et al. 2021). However, as the inner radius of the annular pool decreases, the threshold Marangoni number increases at the same aspect ratio. It means that thermal convection could be weakened when the heating surface becomes smaller, which has been discussed by Tian et al. (2020). At the same aspect ratio and radial temperature difference, the smaller heating surface provides less energy so that the thermal convection becomes more stable.

A power exponential function form is used to clarify the general relationship among these control dimensionless parameters by fitting the present and previous data, as shown in Fig. 3. As a result, the growth of the threshold Marangoni number with the Prandtl number can be characterized by the complex $Ma \times Pr^{-0.6}$, which can be correlated to the dynamic Bond number and the radius ratio by the following equation

$$Ma \times Pr^{-0.6} = 3235.64 \times \left(Bd \times \eta^{0.5}\right)^{0.66} \tag{5}$$

The fitting data obtained from the general relationship is in close accordance with the experimental results, and the adjusted R-square value is 96%.

Figure 4 depicts the evolution of the temperature distributions on the free surface with the increasing radial temperature difference at $Pr = 6.7$ when the depths of the annular pools are respectively 4 mm and 5 mm. When the temperature difference is 25 ℃ ($Ma = 2.2 \times 10^4$), a rotating

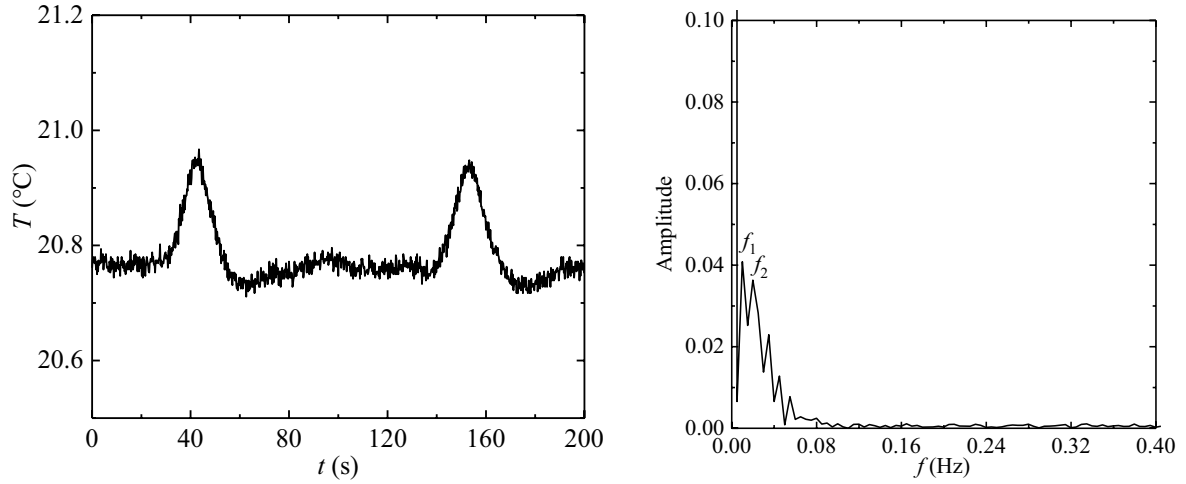

(a) d=5 mm (Bd=3.12), ΔT=22 ºC, Ma=3.06×10^4

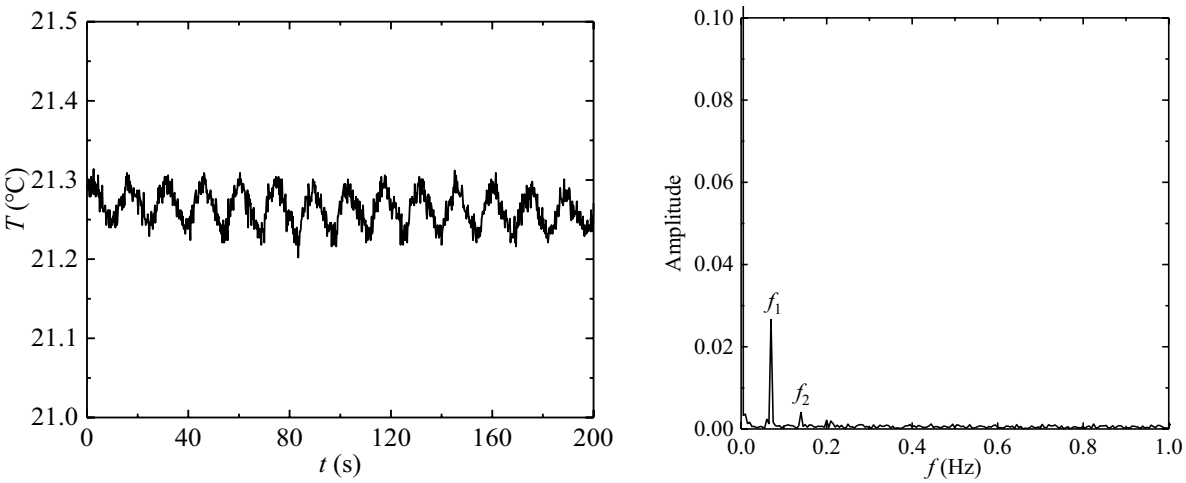

(b) d=6 mm (Bd=4.50), ΔT=19 ºC, Ma=3.80×10^4

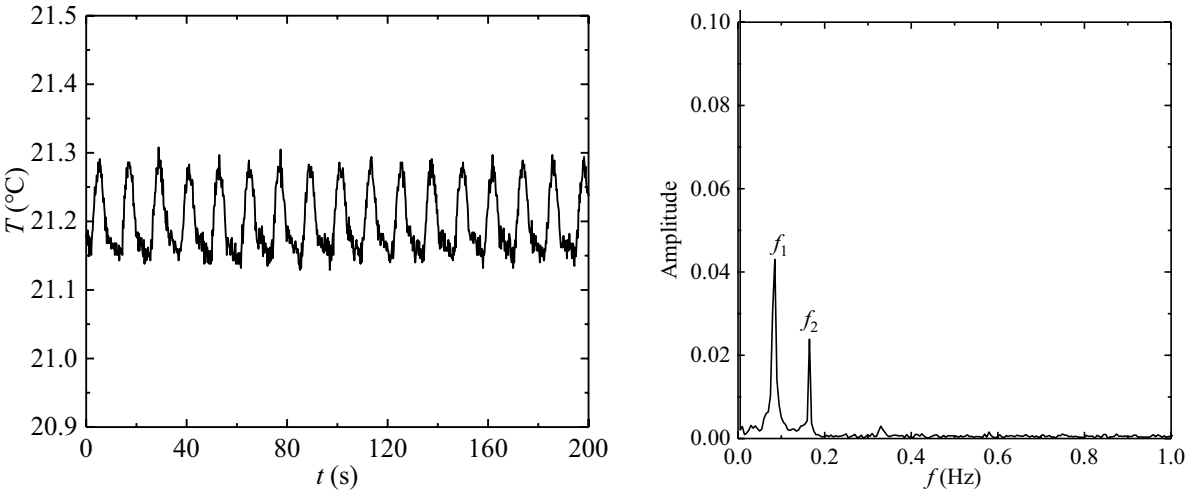

(c) d=7 mm (Bd=6.12), ΔT=19 ºC, Ma=5.18×10^4

Fig. 7 The dependence of the temperature fluctuation (left) and the corresponding FFT diagram (right) at the monitor point 9 on the liquid layer when Pr = 6.7. **a** $f_1 = 0.010, f_2 = 0.020 = 2f_1$; **b** $f_1 = 0.070, f_2 = 0.140 = 2f_1$; **c** $f_1 = 0.085, f_2 = 0.165 \approx 2f_1$

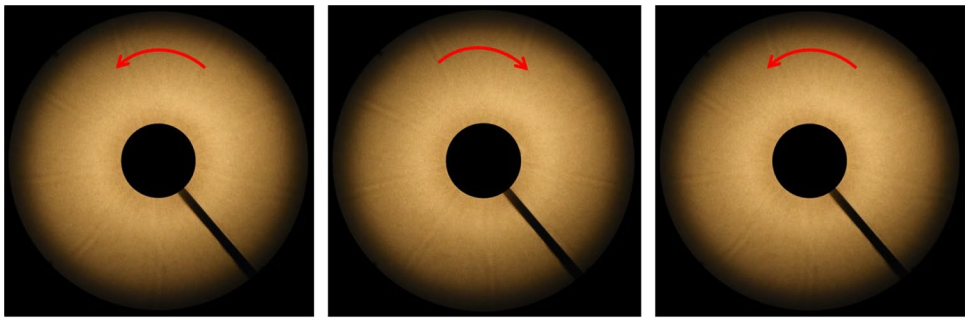

(a) t=0 **(b)** t=T/2 **(c)** t=T

Fig. 8 The oscillating spoke pattern at ΔT = 19 ℃, Ma = 3.80 × 10.^{4}, Pr = 6.7 and d = 6 mm (Bd = 4.50). The oscillation period T is 14.3 s

petal-like structure with the wavenumber of 9 (marked by red number) can be observed firstly in the annular pool with the depth of 5 mm (Γ = 0.17), as shown in Fig. 4b. But, the flow weakens at the depth of 4 mm (Γ = 0.13), and the azimuthal temperature fluctuation is so small that it is difficult to be observed. When the radial temperature difference increases to ΔT = 30 ℃ (Ma = 2.7 × 10^4), a rotating petal-like structure (RPS) with the wavenumber of 10 becomes very clear, as shown in Fig. 4a. When the radius ratio is 0.5, Shu et al. (2021) also reported the slender and short spoke pattern in annular pools with the depth of 4–5 mm. As the Marangoni number increases, they observed a flow pattern transition from the slender and short spokes to petal-like structures. However, in the present work, this transition phenomenon disappears because of the reducing radius ratio. As the radius ratio decreases, the shape of the petal-like structure near the outer cylinder becomes thin and sharp, which is more like a thin and long spoke. Schwabe (2006) also observed similar flow patterns in the circular containers heated from below.

Figure 5 shows the variation of the wavenumber of the flow pattern with the Marangoni number when the fluid depth ranges from 4 to 6 mm and the Prandtl number is 6.7. It can be seen that the wavenumber of the flow pattern has a slight decrease from 10 to 9 with the increasing liquid depth at the radius ratio of 0.25. When the radius ratio of the annular pool increases to 0.5, the corresponding wavenumber of the flow pattern ranges from 16 to 19 (Shu et al. 2021), which is approximately twice more than that in the present work. Obviously, the wavenumber of the flow pattern is proportional to the radius of curvature of the inner hot cylinder when the radius of the outer cylinder remains constant, which agrees well with the linear stability results reported by López-Núñez et al. (2020). Besides, when the radius of the outer cylinder changes, the wavenumber of the flow pattern could be associated with the radius ratio. In comparison to the linear stability results reported by Imaishi et al. (2020), the wavenumber of the flow pattern could be reduced when the radius ratio is decreased.

Figure 6 illustrates the evolution of the temperature fields on the free surface with the Marangoni number when the fluid depth increases from 6 to 8 mm. As shown in Fig. 6a, the wavenumber of the spoke pattern decreases from 10 to 9 when the Marangoni number increases. It could be because the enhancing radial flow on the free surface driven by thermocapillary force results in the decrease of the wavenumber. When the liquid depth is increased to 7–8 mm, the flow pattern transits from the spoke pattern (SP) to the cellular structure (CS) (marked by red arrow) with the increase of the Marangoni number, as shown in Fig. 6b and c. However,

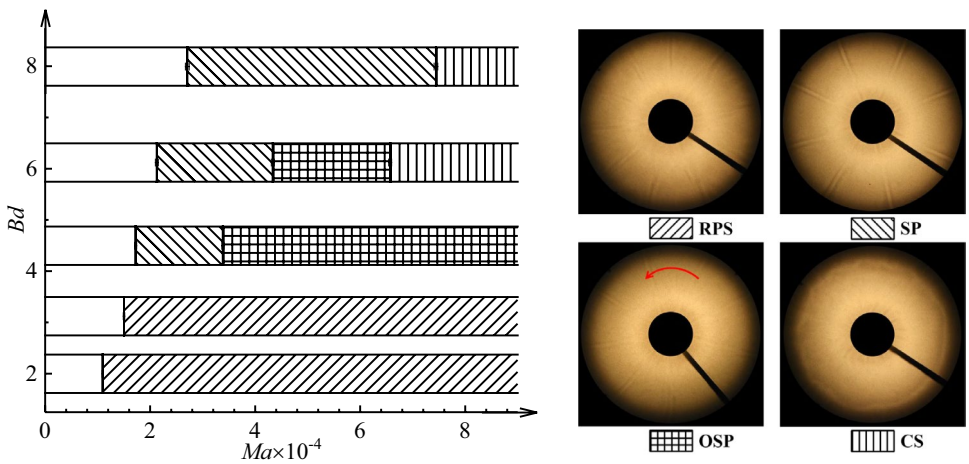

Fig. 9 The influence of the dynamic Bond number on the transitions between various types of convective flows at Pr = 6.7. White block: the basic flow

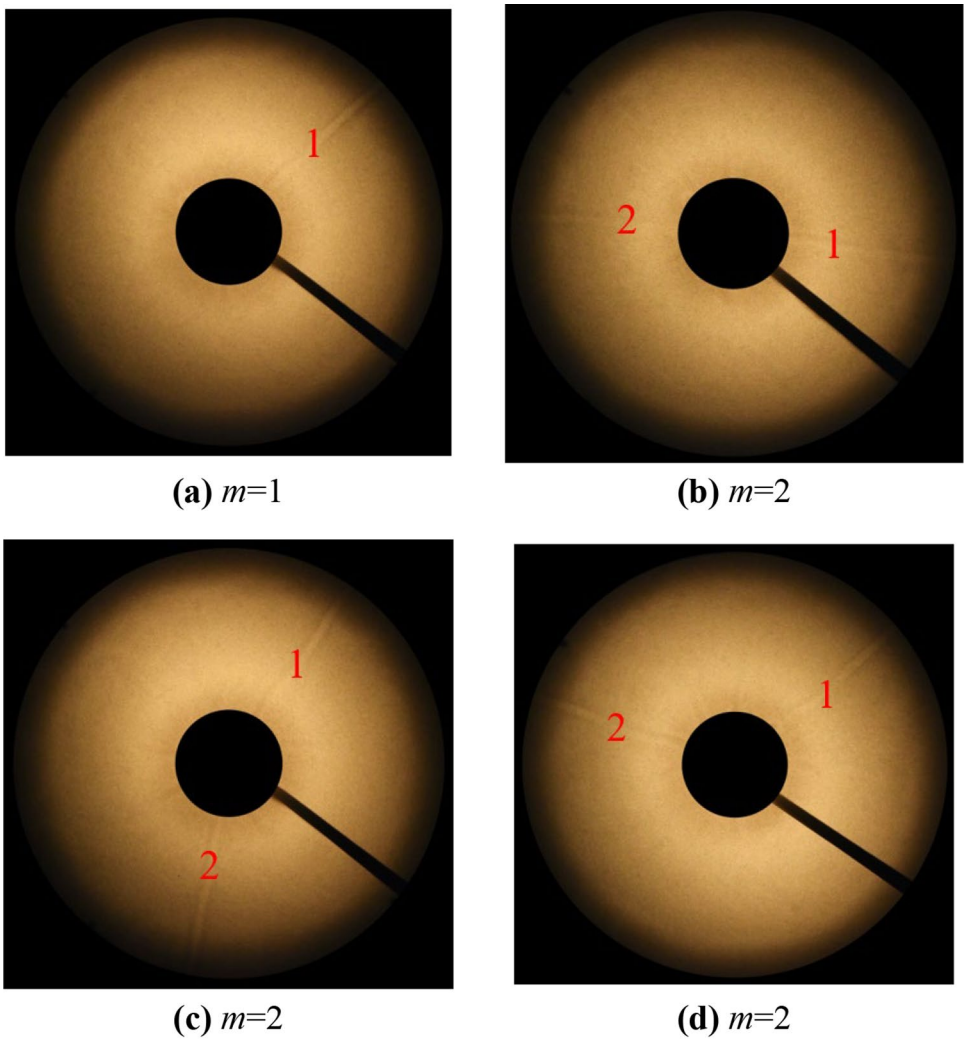

(a) m=1 (b) m=2 (c) m=2 (d) m=2

Fig. 10 The spoke patterns with the wavenumbers of 1and 2 in the annular pool of $d = 7$ mm ($Bd = 6.12$) at $\Delta T = 25$ ℃ ($Ma = 6.8 \times 10^4$) and $Pr = 6.7$

the flow pattern transition has never been observed in the previous work (Shu et al. 2021) in the annular pool with the radius ratio of 0.5. With the decrease of the radius ratio, the heating inner surface decreases and the free surface extends. In this case, the flow pattern in the annular pools becomes more like that in the circular containers heated from below (Schwabe 2006). Therefore, when the liquid depth increases from 6 to 8 mm, the flow pattern transits from the spoke pattern to the cellular structure.

Similar to the previous work (Shu et al. 2021), the flow patterns become oscillating with the increase of the Marangoni number. Especially for the case of d = 6–7 mm, the oscillating spoke pattern (OSP) can be observed when the temperature difference is 19 ℃. As shown in Fig. 7b and c, the characteristic of temperature fluctuation at monitor point 9 is similar to the previous work (Shu et al. 2021). The oscillating spoke pattern, in which all of the spokes alternately swing clockwise and anticlockwise, can be observed in Fig. 8. For $d = 6$ mm and 7 mm, the corresponding periodic oscillation frequency is 0.070 Hz and 0.085 Hz, respectively, which is lower than that in the prior study. It means that the flow becomes weak when the radius ratio is decreased. For this reason, the oscillating petal-like structures can be difficult to be observed during the present experiments. There is only a rotating petal-like structure to be observed in annular pools when the liquid layer thickness is 4–5 mm. As shown in Fig. 0.7a, the petal-like structure rotates so slowly in the annular pools that the oscillating frequency is only 0.010 Hz. The influence of the dynamic Bond number on the evolution of the flow patterns is summarized in Fig. 9.

These similar cellular structures have also been observed in a deep liquid layer heated from below by both numerical simulations (Medale and Cerisier 2015) and experimental investigations (Schwabe 2006). Although the heating mode is different, there are some things in common. One is that the area of the free surface is large enough for generating Bénard-Marangoni convection driven by the surface-tension gradient. The other is that the liquid layer is thick enough for developing the cellular structures in cylindrical containers. Besides, for a thickness liquid layer heated from below, there

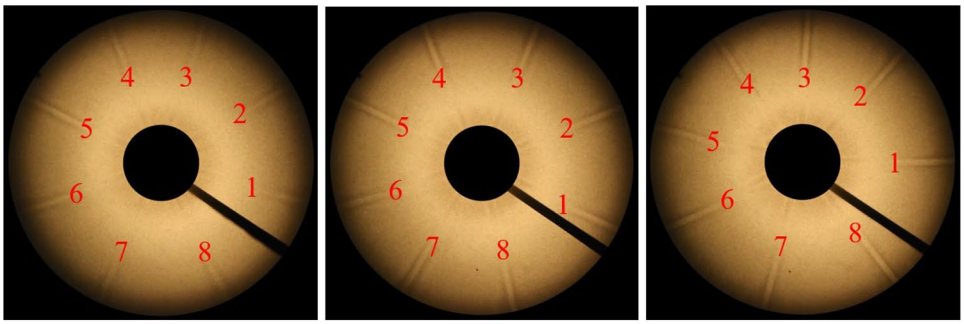

(i) ΔT=30ºC (Ma=5.3×10^4) (ii) ΔT=40ºC (Ma=7.1×10^4) (iii) ΔT=50ºC (Ma=8.9×10^4)

(a) d=6 mm (Bd=4.94)

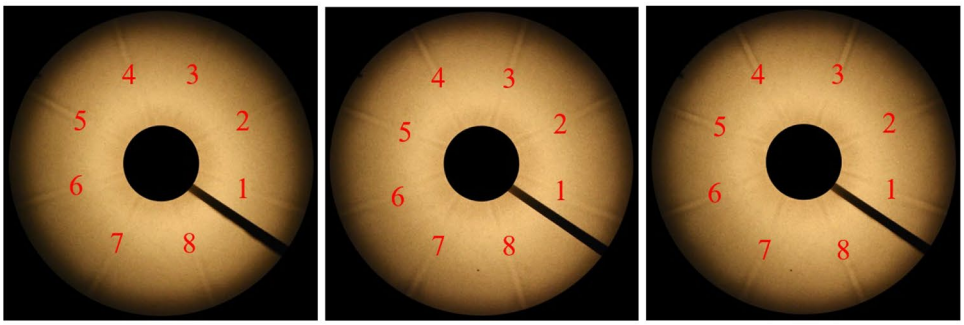

(i) ΔT=30ºC (Ma=7.3×10^4) (ii) ΔT=40ºC (Ma=9.7×10^4) (iii) ΔT=50ºC (Ma=12.1×10^4)

(b) d=7 mm (Bd=6.72)

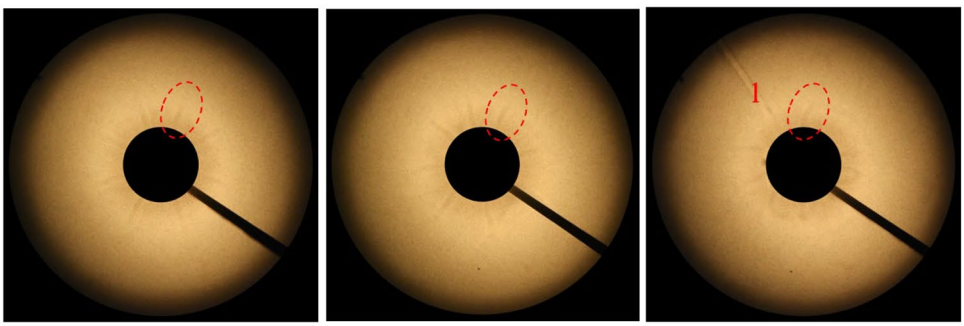

(i) ΔT=30ºC (Ma=9.5×10^4) (ii) ΔT=40ºC (Ma=12.7×10^4) (iii) ΔT=50ºC (Ma=15.9×10^4)

(c) d=8 mm (Bd=8.77)

Fig. 11 Variations of the surface temperature field with the radial temperature difference (Marangoni number) at Pr = 16.1

is only a cellular structure to be observed on the free surface and the main fluid flow direction is from the center to the outside. Similar to the flow direction in the present experiments, the hot fluid ascends along with the inner cylinder and then flows to the outer cylinder.

For the liquid layer with the thickness of d = 7 mm, the wavenumber of the spoke pattern is not a constant number at ΔT = 25 ºC. As shown in Fig. 10, the wavenumber of the spoke pattern converts between 1 to 2 when the experiment is repeated many times under the same condition. Schwabe (2006) also observed a similar phenomenon in circular containers heated from below which is called "mode switching". Under microgravity conditions, they observed that the wavenumber of the spoke-like structures converts between 1 to 2 for circular containers with larger aspect ratios. The "mode switching" is also certified by the linear stability analysis (Hoyas et al. 2013; Rosenblat et al. 1982), but is named as "codimension-two points". The meaning of the codimension-two points is that there are two different wavenumbers under the same experimental condition when the

flow destabilizes. It is evident that the mode switching of the flow patterns can be observed in both the annular pools and the circular containers. Different from the experimental results under microgravity conditions (Schwabe 2006), the buoyancy effect can be neglected; the presented experiments are performed under terrestrial conditions where the dynamic Bond number ranges from 2.0 to 8.0. That is, no matter what the buoyancy effect is absent or exist, the mode switching of the flow patterns always appears. It means that the flow transition from the spoke pattern to cellular structure could be attributed to the thermocapillary effect instead of the buoyancy effect.

Besides, the position of the flow pattern appearance is random during the experiment process. For the spoke pattern with the wavenumber of 2, the waves (marked by red number) are not always evenly distributed in the azimuthal direction of the annular pool, as shown in Fig. 10b-d. Schwabe (2006) has pointed out that the flow pattern is a periodic oscillation and showed the transient behavior of the mode switching. But in the present works, the periodic oscillation becomes difficult to be observed, which could be due to the buoyancy suppression action on the flow.

Figure 11 depicts the evolution of the surface temperature field with the radial temperature difference (Marangoni number) for 1 cSt silicone oil of $Pr = 16.1$. Compared with Fig. 6 at $Pr = 6.7$, the flow transition from the spoke pattern to the cellular structure is difficult to happen. It could be attributed to the increase of the Prandtl number weakening thermocapillary-buoyancy convection. For this reason, when the liquid layer thickness is 6–7 mm, the wavenumber of the spoke pattern maintains at 8 with the increase of the Marangoni number. Besides, for $d = 8$ mm, the cellular structure cannot be observed, there are only the short spokes appear near the inner cylinder (marked by the red dot circle). It should be attributed to the decreasing heating inner surface and the extending free surface. As the Marangoni number increases, the flow is enhanced, and a long spoke can be observed.

Conclusions

A series of terrestrial experiments on thermocapillary-buoyancy convection of 0.65cSt and 1cSt silicone oils have been conducted in annular pools with a smaller heating inner cylinder. Comparisons with the results in the liquid pool with large inner radius are carried out. The main results can be summarized as follows.

1. When the fluid depth is 4–5 mm ($\Gamma = 0.13$–0.17), the rotating petal-like structure appears first on the free surface after the thermocapillary-buoyancy convection destabilizes. At a smaller heating inner radius, the shape of the petal-like structure near the outer cylinder becomes thin and sharp.
2. When the fluid depth is increased to 6–8 mm ($\Gamma = 0.2$–0.27), the spoke pattern appears firstly on the free surface. With the increase of the Marangoni number, the spoke pattern can transit to the cellular structure for the silicone oil of $Pr = 6.7$. Especially, at $d = 7$ mm, a mode switching of the spoke pattern occurs and the wavenumber converts between 1 to 2. As the Prandtl number increases from 6.7 to 16.1, the flow transition from the spoke pattern to the cellular structure can be difficult to happen.
3. At the depth of 6–7 mm, the spoke pattern becomes oscillating as the Marangoni number increases. The periodic oscillating frequency is decreased when the radius ratio is decreased.
4. According to the present and previous experimental results, the general relationship of the threshold complex with the dynamic Bond number and the radius ratio is proposed. The fitting data obtained from the general relationship is in close accordance with the experimental results.

Funding This work is supported by National Natural Science Foundation of China (Grant No. 52076017) and Chongqing University Innovation Research Group Project.

Declarations

Competing Interests The authors declare that they have no known competing financial interests or personal relationships that could have appeared to influence the work reported in this paper.

References

Benz, S., Schwabe, D.: The three-dimensional stationary instability in dynamic thermocapillary shallow cavities. Exp. Fluids. **31**, 409–416 (2001)

Favre, E., Blumenfeld, L., Daviaud, F.: Instabilities of a liquid layer locally heated on its free surface. Phys. Fluids. **9**, 1473–1475 (1997)

Garnier, N., Chiffaudel, A., Daviaud, F.: Hydrothermal waves in a disk of fluid. In: Dynamics of Spatio-Temporal Cellular Structures-Henri Benard Centenary Review, vol. 207, pp. 147–161. Springer, New York (2006)

Hoyas, S., Gil, A., Fajardo, P., Pérez-Quiles, M.J.: Codimension-three bifurcations in a Bénard-Marangoni problem. Phys. Rev. E. **88**, 015001 (2013)

Imaishi, N., Ermakov, M.K., Shi, W.Y.: Effects of Pr and pool curvature on thermocapillary flow instabilities in annular pool. Int. J. Heat. Mass. Transf. **149**, 119103 (2020)

Jing, C.J., Kobayashi, M., Tsukada, T., Hozawa, M., Fukuda, T., Imaishi, N., Shimamura, K., Ichinose, N.: Effect of RF coil position on spoke pattern on oxide melt surface in Czochralski crystal growth. J. Cryst. Growth. **252**, 550–559 (2003)

Kamotani, Y., Ostrach, S., Masud, J.: Microgravity experiments and analysis of oscillatory thermocapillary flows in cylindrical containers. J. Fluid. Mech. **410**, 211–233 (2000)

Li, Y.R., Zhang, L., Zhang, L., Yu, J.J.: Experimental study on Prandtl number dependence of thermocapillary-buoyancy convection in Czochralski configuration with different depths. Int. J. Therm. Sci. **130**, 168–182 (2018)

Liu, H., Zeng, Z., Yin, L.M., Qiu, Z.H., Qiao, L.: Influence of aspect ratio on the onset of thermocapillary flow instability in annular pool heated from inner wall. Int. J. Heat. Mass. Transf. **129**, 746–752 (2019a)

Liu, H., Zeng, Z., Yin, L.M., Qiu, Z.H., Zhang, L.Q.: Effect of the Prandtl number on the instabilities of the thermocapillary flow in an annular pool. Phys. Fluids. **31**, 034103 (2019b)

López-Núñez, E., Pérez-Quiles, M.J., Fajardo, P., Hoyas, S.: Effect of the horizontal aspect ratio on thermocapillary convection stability in annular pool with surface heat dissipation. Int. J. Heat. Mass. Transf. **148**, 119140 (2020)

Malyuk, A.Y., Ivanova, N.A.: Optofluidic lens actuated by laser-induced solutocapillary forces. Opt. Commun. **392**, 123–127 (2017)

Medale, M., Cerisier, P.: Influence of container shape and size on surface-tension-driven Bénard convection. Eur. Phys. J. Spec. Top. **224**, 217–227 (2015)

Miller, D.C., Pernell, T.L.: Fluid flow patterns in a simulated garnet melt. J. Cryst. Growth. **57**, 253–260 (1982)

Mo, D.M., Zhang, L., Ruan, D.F., Li, Y.R.: Aspect ratio dependence of thermocapillary flow instability of moderate-Prandtl number fluid in annular pools heated from inner cylinder. Microgravity. Sci. Technol. **33**, 66 (2021)

Qin, T.R., Tuković, Z., Grigoriev, R.O.: Buoyancy-thermocapillary convection of volatile fluids under their vapors. Int. J. Heat. Mass. Transf. **80**, 38–49 (2015)

Rosenblat, S., Davis, S.H., Homsy, G.M.: Nonlinear Marangoni convection in bounded layers. Part 1. Circular cylindrical containers. J. Fluid. Mech. **120**, 91–122 (1982)

Savino, R., di Francescantonio, N., Fortezza, R., Abe, Y.: Heat pipes with binary mixtures and inverse Marangoni effects for microgravity applications. Acta. Astronaut. **61**, 16–26 (2007)

Schwabe, D.: Marangoni instabilities in small circular containers under microgravity. Exp. Fluids. **40**, 942–950 (2006)

Schwabe, D., Scharmann, A., Preisser, F., Oeder, R.: Experiments on surface tension driven flow in floating zone melting. J. Cryst. Growth. **43**, 305–312 (1978)

Schwabe, D., Zebib, A., Sim, B.C.: Oscillatory thermocapillary convection in open cylindrical annuli. Part 1. Experiments under microgravity. J. Fluid. Mech. **491**, 239–258 (2003)

Shi, W.Y., Ermakov, M.K., Imaishi, N.: Effect of pool rotation on thermocapillary convection in shallow annular pool of silicone oil. J. Cryst. Growth. **294**, 474–485 (2006)

Shi, W.Y., Ermakov, M.K., Li, Y.R., Peng, L., Imaishi, N.: Influence of buoyancy force on thermocapillary convection instability in the differentially heated annular pools of silicon melt. Microgravity. Sci. Technol. **21**, S289–S297 (2009)

Shu, Q., Zhang, L., Mo, D.M., Li, Y.R.: Experiments on thermocapillary-buoyancy convection of medium Prandtl number liquids in annular pools heated from inner cylinder. Int. J. Heat. Mass. Transf. **179**, 121719 (2021)

Tian, Z.A., Zeng, Z., Liu, H., Yin, L.M., Zhang, L.Q., Qiao, L.: Linear stability analysis of thermocapillary flow in rotating shallow pools heated from inner wall. J. Therm. Sci. **29**, 251–259 (2020)

Yu, J.J., Zhang, L., Li, Y.R., Chen, J.C.: Numerical simulations of thermocapillary flow of a binary mixture with the soret effect in a shallow annular pool. Microgravity. Sci. Technol. **28**, 1–10 (2016)

Zhang, L., Li, Y.R., Wu, C.M.: Effect of surface heat dissipation on thermocapillary convection of low Prandtl number fluid in a shallow annular pool. Int. J. Heat. Mass. Transf. **110**, 460–466 (2017)